Electronic Supplementary information (ESI)

For

Oxidation-driven self-assembly gives access to high-nuclearity molecular copper vanadium oxide clusters

Johannes Forster, Benedikt Rösner, Rainer H. Fink, Leanne C. Nye, Ivana Ivanovic-Burmazovic, Katharina Kastner, Johannes Tucher and Carsten Streb*

Department Chemistry and Pharmacy, Friedrich-Alexander-University Erlangen-Nuremberg, Egerlandstr. 1, 91058 Erlangen, Germany.
*Email: carsten.streb@chemie.uni-erlangen.de

1. Instrumentation

X-ray diffraction: Single-crystal X-ray diffraction studies were performed on a Nonius Kappa CCD Single-crystal X-ray diffractometer equipped with a graphite monochromator using MoKα radiation (wavelength λ(Mo-k_α) = 0.71073Å).

UV-Vis spectroscopy: UV-Vis spectroscopy was performed on a Shimadzu UV-2401PC spectrophotometer, Varian Cary 50 spectrophotometer or Varian Cary 5G spectrophotometer equipped with a Peltier thermostat. All systems were used with standard cuvettes (d = 10.0 mm).

Thermogravimetry analysis (TGA): TGA was performed on a Setaram Setsys CS Evo, 30-1000℃ @ 10K/min, 200 mL/min He, Graphite crucib le 0.5 mL.

Atomic absorption spectroscopy: Atomic absorption spectroscopy analysis was performed on a Perkin Elmer 5100 PC spectrometer.

FT-IR spectroscopy: FT-IR spectroscopy was performed on a Shimadzu FT-IR-8400S spectrometer. Samples were prepared as KBr pellets. Signals are given as wavenumbers in cm^{-1} using the following abbreviations: vs = very strong, s = strong, m = medium, w = weak and b = broad.

Elemental analysis: Elemental analysis was performed on a Euro Vector Euro EA 3000 Elemental Analyzer.

Mass spectrometry (MS): MS measurements were performed on a UHR-TOF Bruker Daltonik (Bremen, Germany) maXis, an ESI-ToF MS capable of resolution of at least

40,000 FWHM. Detection was in negative-ion mode, the source voltage was 4 kV, first skimmer potential: -33 V. The flow rates were 500 µL/hour. The drying gas (N_2) was held at 180 °C. The machine was calibrated prior to every experiment via direct infusion of the Agilent ESI-TOF low concentration tuning mixture, which provided an m/z range of singly charged peaks up to 2700 Da.

Cyclic Voltammetry (CV): CV was performed using an Ivium CompactStat potentiometer. Working electrode: carbon disc electrode, reference electrode, counter electrode: Pt wire. Dry solvents were used with nBu$_4$NPF$_6$ as the electrolyte. Scan rates were between 20 - 100 mV/s

General remarks: All chemicals were purchased from Sigma Aldrich or ACROS and were of reagent grade. The chemicals were used without further purification unless stated otherwise. (nBu$_4$N)$_6$[H$_6$V$_{18}$O$_{42}$] was prepared according to reference S1, (nBu$_4$N)$_4$[V$_4$O$_{12}$] was prepared according to reference S2.

2. Synthetic section:

2.1. Synthesis of **{Cu$_6$V$_{30}$}**: (nBu$_4$N)$_4$[Cu$_6$V$_{30}$O$_{82}$(NO$_3$)$_2$(CH$_3$CN)$_6$] x solvent:
(nBu$_4$N)$_6$[H$_6$V$_{18}$O$_{42}$] (200 mg, 66.4 µmol) and Cu(NO$_3$)$_2$·3H$_2$O (101 mg, 418 µmol) were dissolved in 15 ml acetonitrile. The resulting solution was vigorously stirred for one hour at ambient temperature. Diffusion of diethyl ether into the reaction mixture over a period of *ca.* 1 week gave brown needle crystals, which were suitable for X-ray diffraction. Yield: 117 mg (25.7 µmol, 36.8 % based on Cu).
Elemental analysis for the dried compound (all acetonitrile molecules removed) C$_{64}$Cu$_6$H$_{144}$N$_6$O$_{88}$V$_{30}$ in wt.-% (calcd.): C 18.17 (17.81), H 3.93 (3.36), N 1.53 (1.95), Cu 8.97 (8.83), V 35.63 (35.40).
Characteristic UV-Vis signals (in acetonitrile): λ_{max1} = 769 nm (shoulder), ε = 3.22 x 10^2 M^{-1} cm^{-1}. λ_{max2} = 224 nm, ε = 1.35 x 10^6 M^{-1} cm^{-1}

2.2. Reaction under inert atmosphere: The reaction under N_2 atomsphere was conducted as described above (2.1.), but de-aereated acetonitrile was used under nitrogen to exclude oxygen / air from the reaction.

2.3. High quality single crystal synthesis of **{Cu_6V_{30}}**:

(nBu$_4$N)$_4$[V_4O_{12}] (99 mg, 72.5 µmol), (nBu$_4$N)$_6$[$H_6V_{18}O_{42}$] (225 mg, 73.8 µmol) and $Cu(NO_3)_2 \cdot 3H_2O$ (235 mg, 972.6 µmol) were dissolved in 13 ml acetonitrile. The resulting solution was vigorously stirred for one hour at ambient temperature. Diffusion of diethyl ether into the clear reaction mixture gave brown needle crystals, which were suitable for X-ray diffraction. Yield: 121 mg (26.5 µmol, 16.4 % based on Cu).

2.4. Synthesis of $[VO(dmso)_5](NO_3)_2$:

(nBu$_4$N)$_6$[$H_6V_{18}O_{42}$] (298 mg, 97.7 µmol) was dissolved in a dimethyl sulfoxide/water mixture (3 ml, 9:1, v:v). To this concentrated nitric acid (65 wt. %, 460 µl, 6.74 mmol) were slowly added. The emerald green solution was stirred at room temperature over night. Diffusion crystallizations were set up using ethyl acetate as diffusion solvent and light blue single crystals were obtained as the only solid product. The crystals were washed with ethyl acetate and dried under vacuum. Yield: 450 mg (775 µmol, 44.2 % based on V).

Elemental analysis for $C_{10}H_{30}N_2S_5VO_{11}$ (Mw: 581.62 g/mol) in wt.-% (calcd.): C 20.75 (20.65), H 5.11 (5.19), N 4.79 (4.82), S 27.96 (27.57).

2.5. Oxidative fragmentation of $[H_6V_{18}O_{42}]^{6-}$ and formation of $[V^{IV}_2V^{V}_8O_{26}]^{4-}$

(nBu$_4$N)$_6$[$H_6V_{18}O_{42}$] (250 mg, 81.7 µmol) was dissolved in a N,N'dimethyl formamide (5 ml). The solution was exposed to air and over a period several days, the solution colour changed from deep green to deep purple. Crystallization of the solution gave deep purple rod crystals. Single-crystal XRD analysis, elemental analysis and FT-IR showed that the material obtained corresponds to [nBu$_4$N]$_4$[$V^{IV}_2V^{V}_8O_{26}$].

2.6. IR-spectroscopy of **{Cu_6V_{30}}**

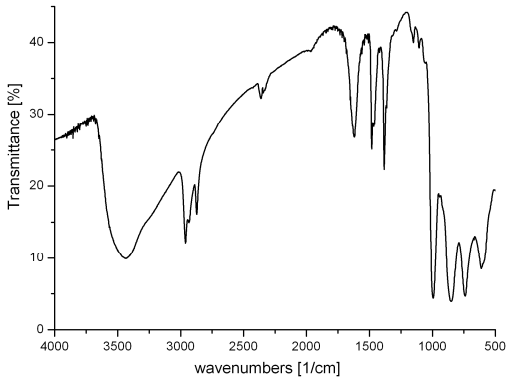

Figure S 1: FT-IR spectrum of **{Cu_6V_{30}}** showing the characteristic V-O vibrational modes in the fingerprint region < 1000 cm^{-1} and the characteristic nitrate-based N-O stretching vibration at 1383 cm^{-1}.[S3]

2.5. UV-Vis spectroscopy

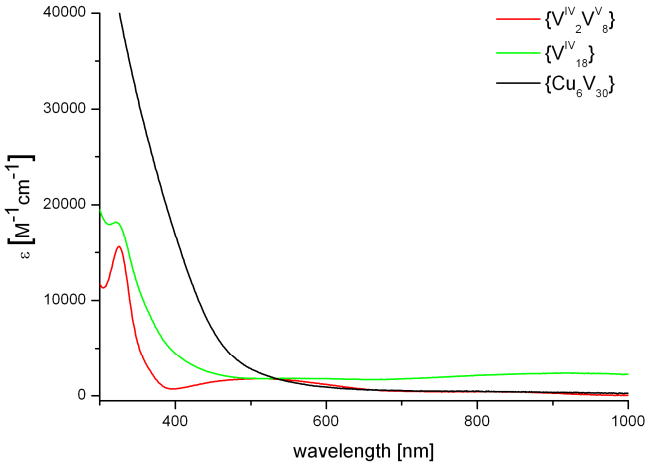

Figure S 2: UV-Vis spectra of the mixed-valent $(nBu_4N)_4[V_{10}O_{26}]$ cluster (= $\{V^{IV}_2V^V_8\}$, red), the fully V^{IV}-based $(nBu_4N)_6[H_6V_{18}O_{42}]$ (= $\{V^{IV}_{18}\}$, green) and **{Cu_6V_{30}}** (black).

3. Crystallographic information

Single-Crystal Structure Determination: Suitable single crystals of the respective compound were grown and mounted onto the end of a thin glass fibre using Fomblin oil. X-ray diffraction intensity data were measured at 150 K on a Nonius Kappa CCD diffractometer [λ(Mo-K_α) = 0.71073 Å] equipped with a graphite monochromator. Structure solution and refinement was carried out using the SHELX-97 package[S4] *via* WinGX.[S5] Corrections for incident and diffracted beam absorption effects were applied using empirical[S6] methods. Structures were solved by a combination of direct methods

and difference Fourier syntheses and refined against F^2 by the full-matrix least-squares technique. Crystal data, data collection parameters and refinement statistics are listed in Table S1. These data can be obtained free of charge via www.ccdc.cam.ac.uk/conts/retrieving.html or from the Cambridge Crystallographic Data Center, 12, Union Road, Cambridge CB2 1EZ; fax:(+44) 1223-336-033; or deposit@ccdc.cam.ac.uk. CCDC reference numbers 890307 (**1**) and 890308 (**2**)

Table S1: Summary of the crystallographic information

	Compound 1	**Compound 2**
Formula	$C_{76}H_{162}Cu_6N_{12}O_{88.67}V_{30}$	$C_{10}H_{30}N_2O_{12}S_5V_1$
M_r g mol^{-1}	4561.64	581.60
crystal system	Trigonal	Triclinic
space group	$P3_121$	P-1
a [Å]	20.411(3)	9.4145(19)
b [Å]	20.411(3)	11.119(2)
c [Å]	40.340(5)	13.183(2)
α [º]	90	67.27(3)
β [º]	90	77.71(2)
γ [º]	120	89.25(3)
V [Å^3]	14554 (3)	1240.0(4)
ρ_{cald} [g cm^{-3}]	1.511	1.558
Z	3	2
μ(Mo$_{K\alpha}$) mm^{-1}	2.084	0.875
T [K]	150(2)	150(2)
no. rflns (measd)	167266	13758
no. rflns (unique)	19763	4904
no. params	839	299
R1 (I>2σ(I))	0.0479	0.0276
wR2 (all data)	0.1222	0.0721
GooF	1.039	1.144
Max/min resd e	0.706/-0.453	0.474/-0.280

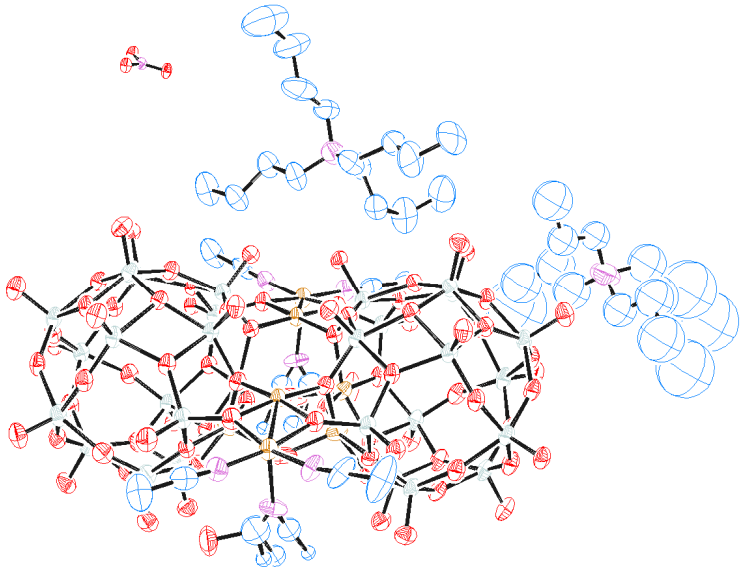

Figure S 3: ORTEP-plot of compound **1**, $(n\mathrm{Bu_4N})_4[\mathrm{Cu_6V_{30}O_{82}(NO_3)_2(CH_3CN)_6}]$, probability ellipsoids given at 50 %. The carbon atoms of the $(n\mathrm{Bu_4N})^+$ tetra-*n*-butylammonium cation based around N6 were refined isotropically due to strong structural disorder. One ligand acetonitrile molecule was heavily disordered and was refined isotropically. The metal oxide cluster atoms were refined fully anisotropically. This allowed refinement of the structure to satisfactory R values.

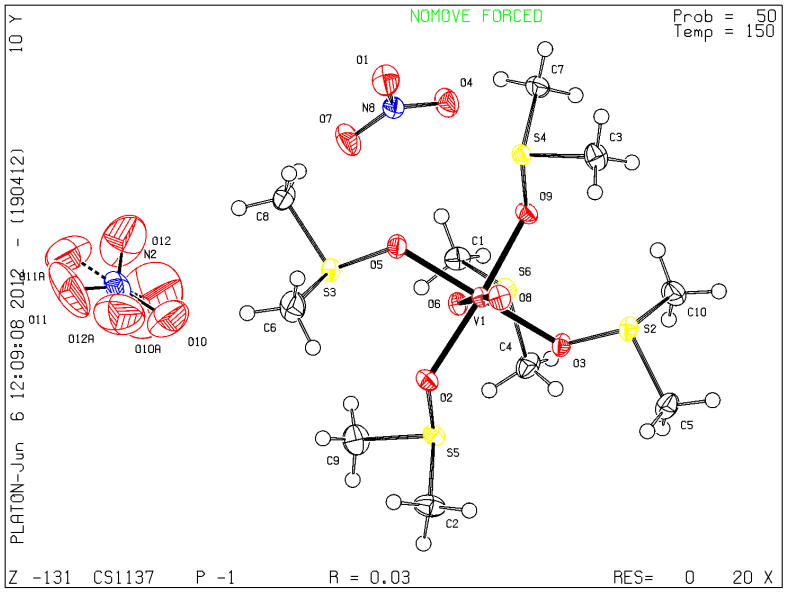

Figure S 4: ORTEP-plot of compound **2**, $[\mathrm{VO(dmso)_5}](\mathrm{NO_3})_2$, probability ellipsoids given at 50 %. All non-hydrogen atoms were refined anisotropically.

4. Mass spectrometry

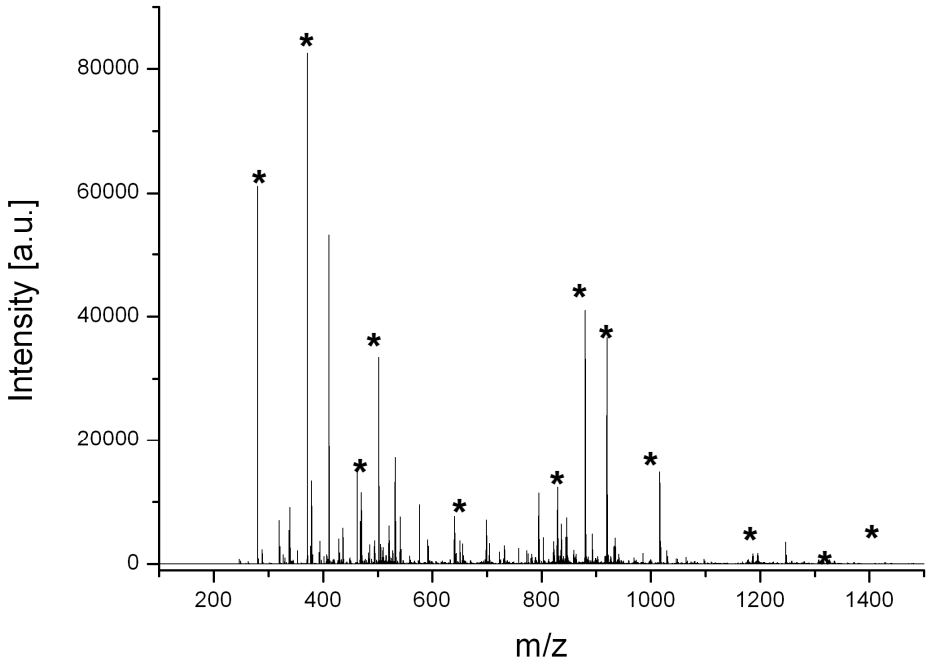

Figure S 5: Negative mode high resolution ESI mass spectrum of **{Cu_6V_{30}}** ([**{Cu_6V_{30}}**] ca. 9 x 10^{-5} M in acetonitrile). Assigned peaks are marked with an asterisk (*)

Table S2: Peak assignments for the ESI mass spectrum of **{Cu_6V_{30}}**

recorded m/z	calculated m/z	peak assignment
280.79[a]	280.79[S8]	$[V_6O_{16}]^{2-}$
371.72[a]	371.72[S8]	$[V_8O_{21}]^{2-}$
462.65[a]	462.65[S8]	$[V_5O_{13}]^{-}$
644.52[a]	644.52[S8]	$[V_7O_{18}]^{-}$
836.34[b]	836.36	$[Cu_6V_{30}O_{82}(NO_3)_2]^{4-}$
941.77	941.77	$(n\mathrm{Bu}_4\mathrm{N})_2[Cu_5V_{30}O_{82}(NO_3)_2]^{4-}$
1016.24[c]	1016.23	$(n\mathrm{Bu}_4\mathrm{N})_2[CuV_{15}O_{40}(NO_3)(H_2O)]^{2-}$
1195.88[b]	1195.91	$(n\mathrm{Bu}_4\mathrm{N})_1[Cu_6V_{30}O_{82}(NO_3)_2]^{3-}$
1336.46[b]	1336.46	$(n\mathrm{Bu}_4\mathrm{N})_3[Cu_5V_{30}O_{82}(NO_3)_2]^{3-}$
1476.31[b]	1476.34	$(n\mathrm{Bu}_4\mathrm{N})_5[Cu_4V_{30}O_{82}(NO_3)_2]^{3-}$

[a] Fragmentation product; [b] full $\{Cu_6V_{30}\}$ cluster anion; [c] $\{CuV_{15}\}$ sub-shell

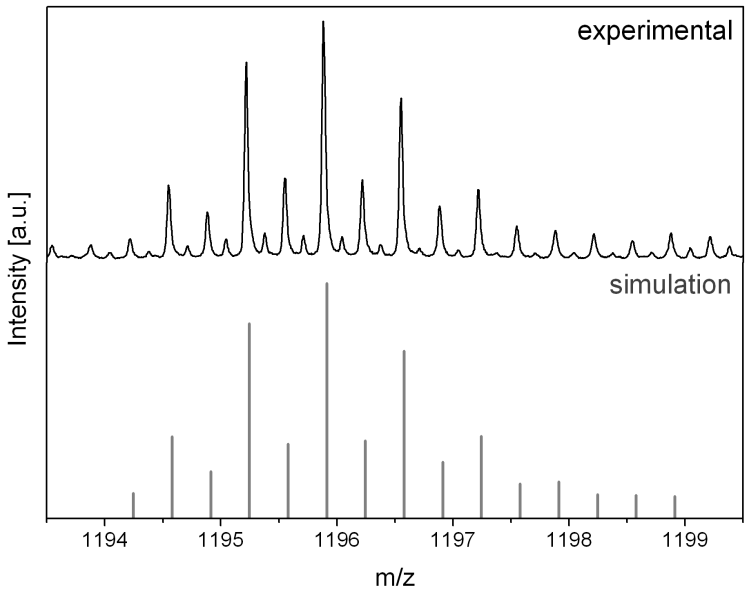

Figure S 6: Experimental and simulated ESI mass spectrum of the full cluster anion $(n\mathrm{Bu_4N})_1[\mathrm{Cu_6V_{30}O_{82}(NO_3)_2}]^{3-}$ at m/z = 1195.88.

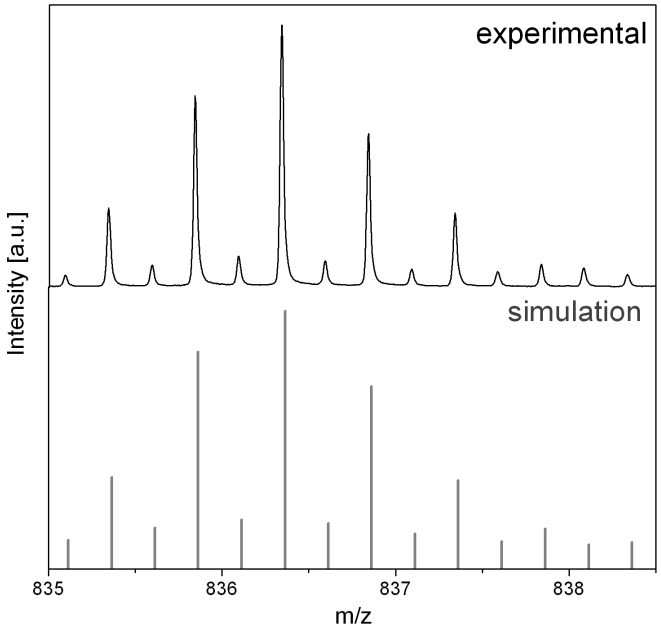

Figure S 7: Experimental and simulated ESI mass spectrum of the full cluster anion $[\mathrm{Cu_6V_{30}O_{82}(NO_3)_2}]^{4-}$ observed at m/z = 836.34.

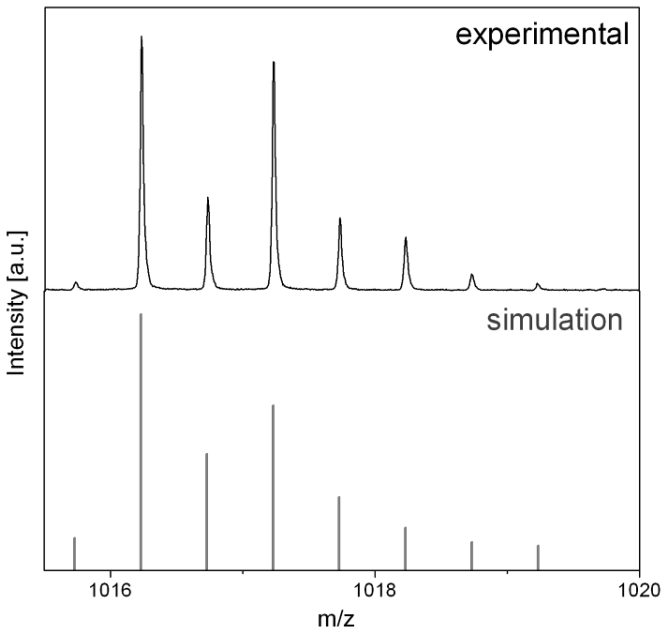

Figure S 8: Experimental and simulated ESI mass spectrum of a $\{CuV_{15}\}$ sub-shell $(n Bu_4N)_2[CuV_{15}O_{40}(NO_3)(H_2O)]^{2-}$ observed at m/z = 1016.24 m/z.

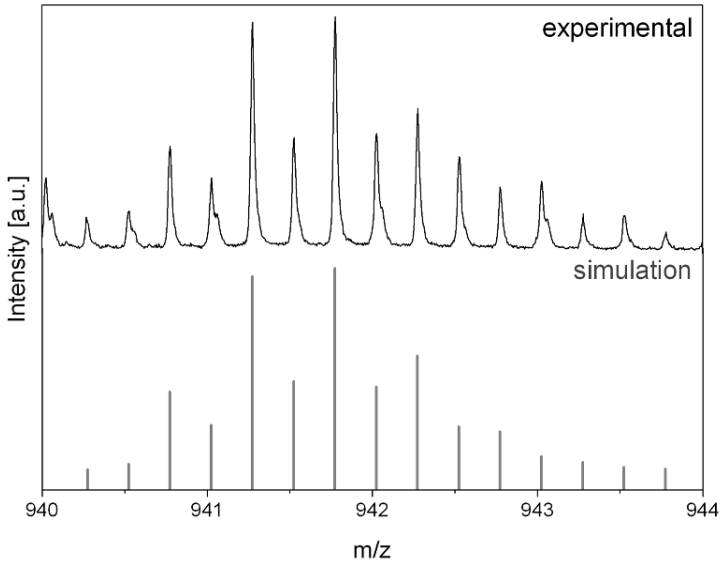

Figure S 9: Experimental an simulated ESI mass spectrum showing the loss of one Cu^{II} centre from the cluster shell: $(n Bu_4N)_1[Cu_5V_{30}O_{82}(NO_3)_2]^{4-}$ observed at m/z = 941.77.

5. Thermogravimetric analysis

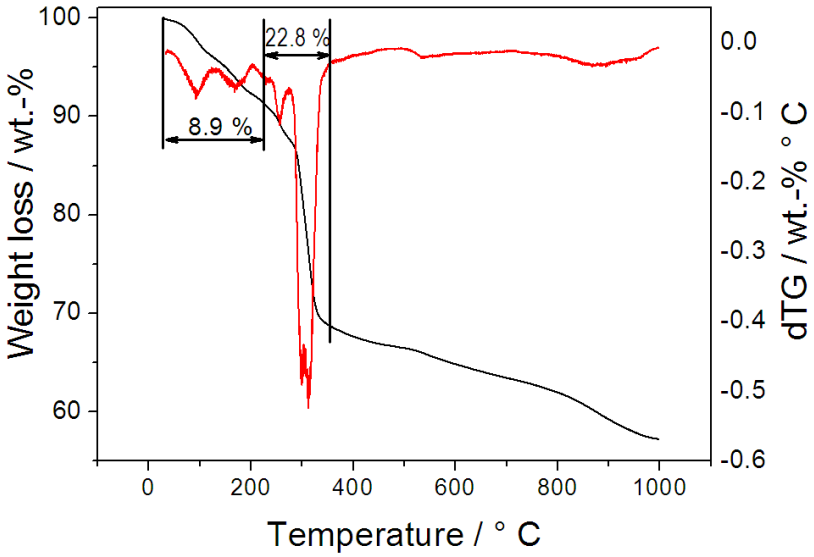

Figure S 10: Thermogravimetric analysis of **{Cu_6V_{30}}** (performed under air, heating rate: 10 ° C /min) showing the loss of adsorbed solvent and water up to T= 200 ° C (weight loss: 8.9 wt.-%) and decomposition of the organic $n$$Bu_4N^+$ cations T= 200 - 350 ° C (weight loss: 22.8 wt.-%, calculated: xy 21.2 wt.-%). At temperatures above 350 ° C, further decomposition of compound 1 is observed.

6. Cyclic Voltammetry

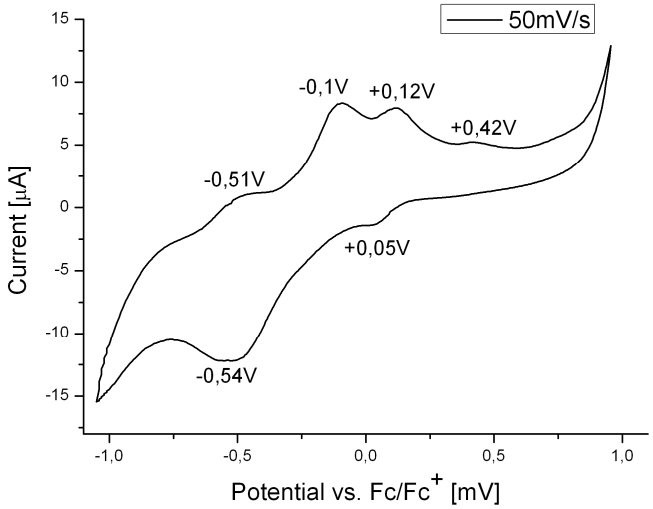

Figure S 11: Cyclovoltammogram of **{Cu_6V_{30}}** (**[{Cu_6V_{30}}** *ca.* 10 mM) in DMF containing 0.1 M ($n$$Bu_4N$)$PF_6$. Scan rate: 50 mV/s, rest potential: -0.4 V.

7. Redox titration

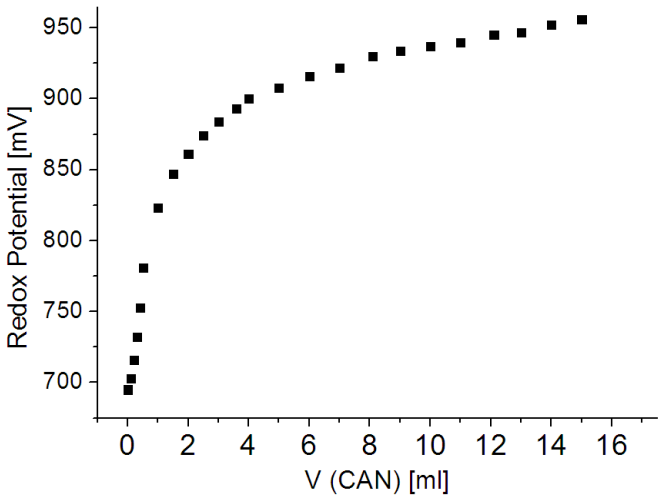

Figure S 12: Redox-titration of **{Cu_6V_{30}}** in DMF ([**{Cu_6V_{30}}**] = 0.1 M) using cerium ammonium nitrate (CAN, 0.05 M) as the oxidant.

8. NEXAFS spectroscopy

Samples for NEXAFS spectroscopy were prepared by suspending the material under investigation in a small amount of ethanol and depositing the suspension on the support. Samples were dried under vacuum to remove excess solvent.

NEXAFS spectroscopy on {Cu_6V_{30}}, {V_{10}} and {V_{18}} clusters was performed as described in the experimental section of the paper. The spectra were normalized to define the pre-edge region as 0 and the edge jump as 1. It has to be noted that this normalization contains the vanadium L_3-edge, the vanadium L_2-edge as well as the oxygen K-edge. The spectra were fitted to a sigmoidal function for the edge jump and Gaussian functions for the near-edge resonances to chi-square values of 0.06, 0.04 and 0.023 (due to a higher noise level). The energy position of the first fitted Gaussian was taken as a direct measure for the oxidation state of the vanadium contained in the cluster as known from the literature.[S9] It has been found that the {Cu_6V_{30}} cluster shows the first resonance at 518.6 eV, which is typical of vanadium (V). The reference spectra (Fig. S 14 and S 15) confirm this finding since the first resonance peak in the {V_{18}} cluster is at a much lower energy at 517.3 eV.

A NEXAFS spectrum of the copper L_3-edge was recorded in the same way in order to confirm the oxidation state +II. The main resonance peak is again in agreement with

copper (II). A copper (I) reference (Cu-TCNQ) and at the literature confirm these findings.[S10]

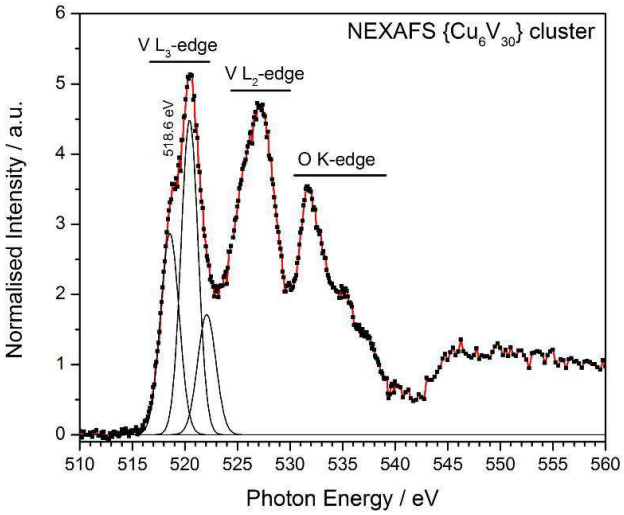

Figure S 13: NEXAFS spectrum of **{Cu_6V_{30}}**.

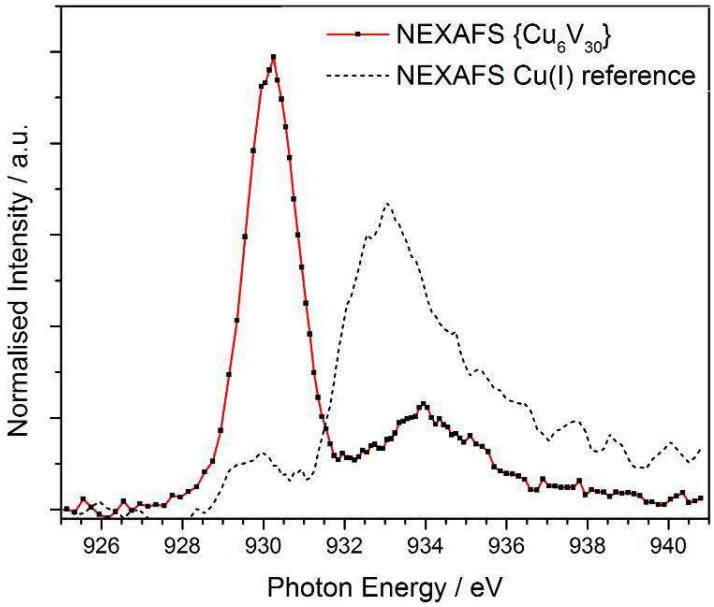

Figure S 14: NEXAFS spectrum of **{Cu_6V_{30}}** and Cu^{I} reference spectrum using Cu^{I}TCNQ as reference compound.

9. Literature references cited in ESI

S1 A. Müller, R. Sessoli, E. Krickemeyer, H. Bögge, J. Meyer, D. Gatteschi, L. Pardi, J. Westphal, K. Hovemeier, R. Rohlfing, J. Döring, F. Hellweg, C. Beugholt, M. Schmidtmann, *Inorg. Chem.* **1997**, *36*, 5239-5250.

S2 J. Forster, B. Rösner, M. M. Khusniyarov, C. Streb, *Chem. Commun.* **2011**, *47*, 3114-3116.

S3 Hesse, M., Meier, H., Zeeh B. *Spektroskopische Methoden in der organischen Chemie*, **2005**, Vol. 7, 57.

S4 G. M. Sheldrick, Acta Crystallogr. **2008**, *A64*, 112.

S5 L. J. Farrugia, J. Appl. Crystallogr. **1999**, *32*, 837.

S6 R. H. Blessing, Acta Crystallogr. **1995**, A*51*, 33.

S7 P. Coppens, L. Leiserowitz, D. Rabinovich, Acta Crystallogr. **1965**, *18*, 1035.

S8 T. McGlone, J. Thiel, C. Streb, D. L. Long, L. Cronin, Chem. Commun. **2012**, *48*, 359-361.

S9 J. G. Chen, C. M. Kim, B. Frühberger, B. D. Devries and M. S. Touvelle, *Surf. Sci.* **1994**, *321*, 145-155.

S10 A. B. Gurevich, B. E. Bent, A. V. Teplyakov, J. G. Chen, *Surf. Sci.* **1999**, *442*, L971-L976.